Experimental Study on the Wettability of Coal with Different Metamorphism Treated by Surfactants for Coal Dust Control

Xiaoxue Liao,[§] Bo Wang,[§] Liang Wang,* Jintuo Zhu,* Peng Chu, Zibin Zhu, and Siwen Zheng

ACCESS | Metrics & More | Article Recommendations

ABSTRACT: Wet dedusting is the main coal dust suppression technique in coal mines, and coal wettability is the main factor affecting dust suppression efficiency. To investigate the main factors affecting the coal wettability and improve it, the coal−water contact angle was used as an index to characterize the coal wettability, and the wettability of six coal samples with different metamorphic degree was studied by analyzing the relationship between the physicochemical properties and the contact angle. To improve the coal wettability, the nonionic surfactant alkyl polyglycoside (APG), anionic surfactant sodium dodecyl benzene sulfonate (SDBS), and polymer surfactant polyacrylamide (PAM) were applied to the coal samples. The results show that SDBS is the most effective surfactant to improve the coal wettability, followed by APG, while the application of PAM would lead to more hydrophobic coal. It is also found that the coal wettability shows a high−low−high trend with the increase in the metamorphic degree. The wettability of long flame coal is the strongest and that of gas coal is the weakest. Moisture is the main hydrophilic factor of coal, while 1,4-dimethylbenzene is the main hydrophobic factor. The main factors affecting the treatment effect of APG, SDBS, and PAM on wettability are the aromatic methylbenzene, hydroxyl, and hydroxyl content of coal, respectively. Therefore, according to the content of hydroxyl in different coals, an SDBS solution can be prepared to improve the coal wettability. For coal with a low hydroxyl content, a higher concentration SDBS solution could be needed.
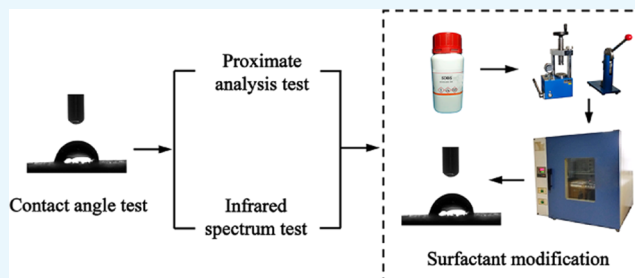
1. INTRODUCTION

Coal is one of the leading energy and an indispensable fuel for the development of the global industry. In China, from 2012 to 2019, the average annual production of raw coal accounts for more than 68% of the primary energy, and the total consumption of coal accounts for more than 57% of the total energy consumption. However, with the improvement of mechanization and automation in coal mining, the dust pollution in coal mines becomes more and more serious, which severely threatens the miners' safety and health.[1,2] Coal dust can not only cause explosions but also lead to pneumoconiosis in coal miners, which is the highest morbidity occupational disease in China.[3,4] To reduce the coal dust disaster, it is necessary to take effective measures to control the dust concentration in coal mines.

Currently, wet dedusting methods such as spray dust suppression, water injection, and foam dust reduction are the main dust control measures in coal mines.[5−9] However, due to the poor wettability of some coal dust, the wet dedusting efficiency is not ideal. Generally, coal wettability is characterized by the coal−water contact angle.[10−14] The smaller the contact angle, the better the coal wettability, and the more hydrophilic the coal.[15] Recently, the addition of surfactants or ionic liquids to water was reported by some scholars as an effective way to reduce the interfacial tension between coal and water, thus improving the coal wettability.[16,17] To reduce the coal−water

contact angle, Ni et al.[18] added a certain concentration of imidazoline ionic liquids into distilled water and it was found that the coal wettability was improved. Wang et al.[19] investigated the influence of anionic and nonionic surfactants on coal wettability and concluded that the anionic surfactants can better improve the wettability of coal in water. Jiang et al.[20] and Ni et al.[21] found that adding sodium chloride (NaCl) to a sodium dodecyl sulfonate solution (SDS) can improve the wettability of coal in a surfactant solution, and the higher the NaCl concentration, the better the coal wettability. Zhou et al.[22] mixed an anionic surfactant with a cationic surfactant and then magnetized the mixed solution, which significantly improved the wettability of coal dust in water. Sang et al.[23] mixed SDS, kerosene, ethanol, and distilled water and developed a microemulsion that can wet coal dust more easily than traditional wetting agents such as SDS and water. To improve the coal wetting effect of coal seam water injection, Ma et al.[24] synthesized
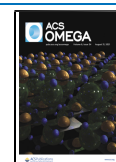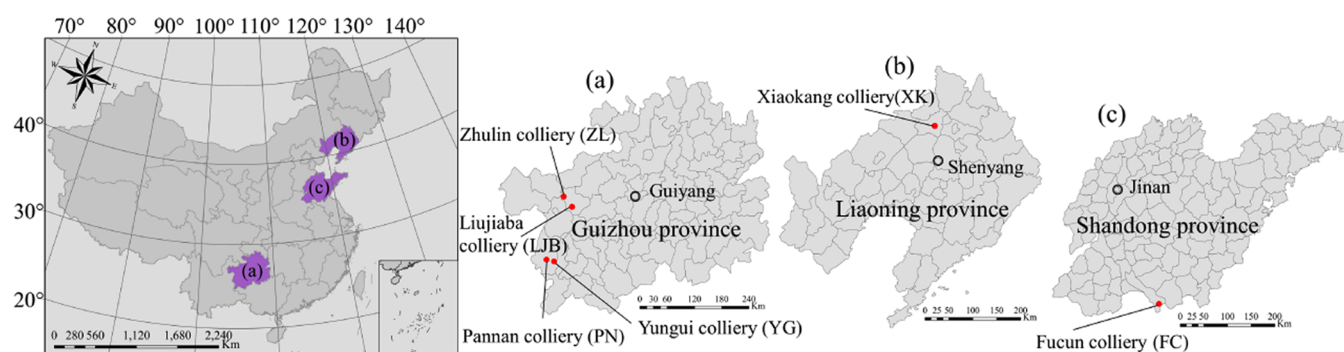
Figure 1. Information of six sampling locations. (a) Guizhou province. (b) Liaoning province. (c) Shandong province.
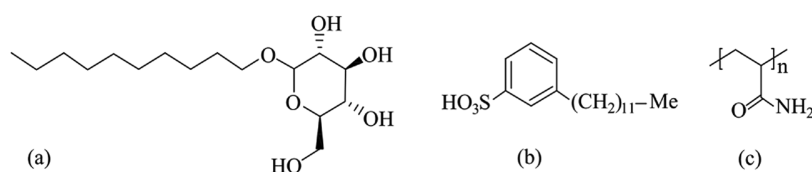

Figure 2. Molecular structure formula of selected surfactants. (a) APG. (b) SDBS. (c) PAM.

Table 1. Information on the Required Particle Sizes and Instruments for Different Testing Objectives

| objective	test	particle size (mm)	instrument
proximate analysis indexes	proximate analysis	0.074−0.2	5E-MVC6700 automatic proximate analyzer (Changsha Kaiyuan Instruments, China)
metamorphic degree	average maximum reflectance of vitrinite test	0.2−0.25	Microscope photometer (Zeiss, Germany)
functional group	infrared spectrum test	<0.074	FTIR-650 Fourier transform infrared spectrometer (Beijing Global Hengda Technology Co., Ltd.)
wettability	contact angle test	<0.074	SCI4000B automatic dynamic contact angle measuring instrument (Beijing Global Hengda Technology Co., Ltd.)
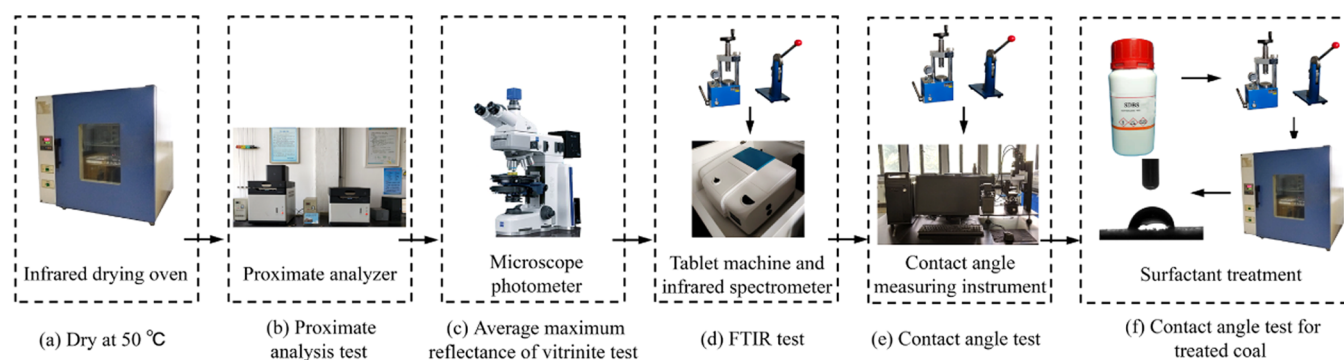
Figure 3. Schematic diagram of testing instruments and the process. (a) Dry at 50 °C. (b) Proximate analysis test. (c) Average maximum reflectance of the vitrinite test. (d) FTIR test. (e) Contact angle test. (f) Contact angle test for treatment coal.

a new water injection additive with β−cyclodextrin as a raw material, which could effectively reduce the coal−water contact angle and improve the dust reduction efficiency. Yang et al.[25] and Wang et al.[26] added a cationic surfactant to the viscoelastic surfactant fracturing fluid, causing a decrease in interfacial tension between coal and liquid in the process of coal seam water injection, thus improving the coal wettability. However, since both the chemical structure and the concentration of the surfactant and the physicochemical properties of coal can affect the coal wettability, the most suitable surfactant for different coals also varies.[27]
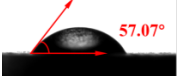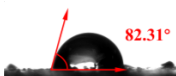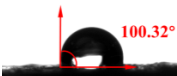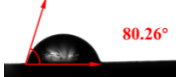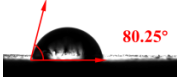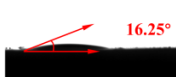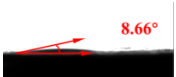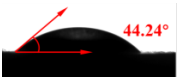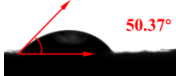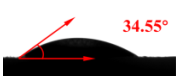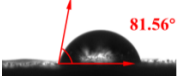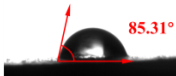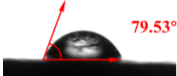
Based on the nuclear magnetic resonance experiments, Zheng et al.[28] investigated the microscopic mechanism of nine different types of surfactants affecting coal wettability and

concluded that phenol, aryl ether carbon, aliphatic, and aromatic methyl groups are the key parameters affecting coal wettability. Zhou et al.[29] established the evaluation index system of wetting parameters by an analytic hierarchy process and proposed a method to obtain the optimum surfactant concentration for spray dust suppression. According to Fourier transform infrared spectroscopy (FTIR), Ma et al.[30] and Xu et al.[31] investigated the effect of the chemical structure of a surfactant and concluded that hydroxyl is the hydrophilic factor and the aliphatic group is the hydrophobic factor of coal. To better improve the effect of the surfactant on coal wettability, some scholars further studied the internal factors affecting coal wettability. Arif[32,33] reported that coal wettability increases with the decrease in the metamorphic

Table 2. Basic Physical Parameters and Contact Angle Testing Results

coal sample	coal category	R_o (%)	proximate analysis index (wt %)				contact angle (deg)			
			M_{ad}	A_{ad}	V_{daf}	FC_{ad}	distilled water	APG	SDBS	PAM
LJB	anthracite	2.69	2.66	15.58	8.44	75.95	16.26	13.79	10.12	57.07
PN	coking coal	1.67	0.94	13.66	16.25	73.59	82.31	19.11	16.63	100.32
ZL	fat coal	1.13	0.89	4.24	20.38	76.22	80.26	24.59	8.29	80.25
XK	long flame coal	0.63	10.62	34.52	44.47	41.09	16.25	8.66	8.25	44.24
YG	meager coal	1.83	1.34	20.54	11.98	71.06	50.37	34.55	26.34	81.56
FC	gas coal	0.98	1.84	11.4	35.36	59.46	85.31	30.58	11.65	79.53

Table 3. Contact Angle of Coal Samples

coal sample	contact angle of coal treated by different surfactant solution			
	distilled water	APG	SDBS	PAM

degree and the ζ potential of coal. Hongchao et al.[34] reported that the moisture, ash, oxygen-containing functional groups, and hydroxyl groups of coal can improve the coal wettability, while the aromatic hydrocarbons can weaken the coal wettability and affect the synergistic acidification of SDS and coal. However, Xu et al.[35] concluded that moisture can improve coal wettability, while ash, volatile matter, and fixed carbon do not affect the coal wettability. Wang et al.[36] analyzed the relationship between functional groups obtained by FTIR and the contact angle of respirable coal dust, and concluded that oxygen-containing functional groups are hydrophilic factors and aromatic hydrocarbons and aliphatic hydrocarbons are hydrophobic factors. Semenova[37] studied the chemical structure of coal with different metamorphic degrees and concluded that the higher the content of hydroxyl and carboxyl, the better the coal wettability. Shi et al.[38] indicated that the pore structure, ash, and minerals are the main factors to improve the wettability of magmatic intrusive coal. In summary, all of the concentrations and structures of surfactants and the physicochemical properties of coal are influencing factors of the coal wettability. Adding suitable surfactants into the water and injecting the solution into the coal seam can improve the coal wettability, and then the floating coal dust with modified wettability and produced during coal mining process can be more efficiently captured by the water spray. To improve the coal wettability, it is necessary to investigate
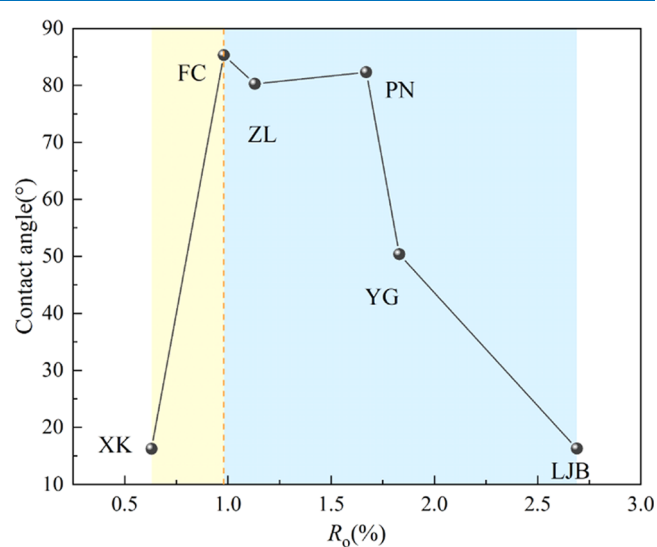
Figure 4. Relationship between the contact angle and metamorphic degree.

its main affecting factors so as to provide guidance for the preparation and selection of wetting agents.
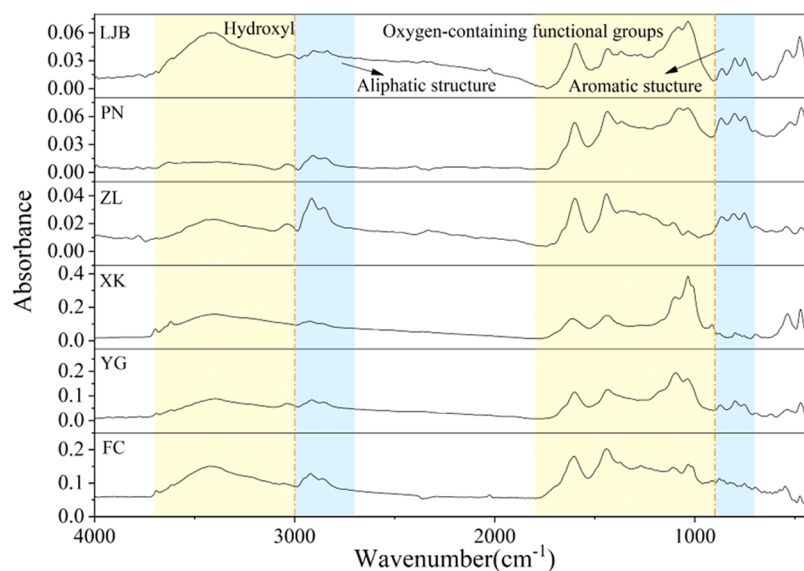
Figure 5. Original infrared spectrum of coal samples.

Figure 6. Fitting results of the infrared spectrum for 3000−3700 cm^{-1}. (a) LJB. (b) PN. (c) ZL. (d) XK. (e) YG. (f) FC.

Therefore, we collected coal samples with different metamorphic degrees from six coal mines in China. The coal wettability was characterized by the coal−water contact angle. The physical properties and the chemical functional group structure of coal were tested, and the main factors affecting the coal wettability were calculated by the grey system theory model. Then, different surfactants were applied to treat the coal samples to improve the coal wettability, and the main factors affecting the treatment effect of surfactants on coal wettability were analyzed.

2. EXPERIMENTS AND METHODS

2.1. Coal Samples and Surfactants. According to the Chinese National Standard GB/T 482−2008, six coal samples with different metamorphic degrees were collected from

Guizhou, Shandong, and Liaoning provinces of China. The detailed sampling locations are shown in Figure 1. To improve the coal wettability, alkyl polyglycoside (APG), sodium dodecyl benzene sulfonate (SDBS), and polyacrylamide (PAM) were applied to improve the wettability of coal samples. APG is an environmentally friendly and safe nonionic surfactant, SDBS is an anionic surfactant, and PAM is a polymer surfactant. Figure 2 shows the molecular structure formulae of these three surfactants.

2.2. Experimental and Analytical Methods. *2.2.1. Experiments.* The coal samples were crushed and sieved into different required particle sizes for different testing objectives, and then dried in a constant temperature drying oven at 50 °C for 24 h to remove the external moisture of coal. The relevant

testing information is listed in Table 1. The average maximum reflectance of vitrinite, the proximate analysis indexes (internal moisture, ash, volatile, and fixed carbon percentage content), and the Fourier transform infrared spectroscopy (FTIR) were tested according to the Chinese national standard GB/T 6948−2008, GB/T 212−2008, and GB/T 6040−2019, respectively. The infrared spectrum test range is 4000−400 cm^{-1}, the resolution is 4 cm^{-1}, and the scanning times are 32. The functional group information of coal was obtained by the potassium bromide tablet pressing method.[39]

Referring to the literature,[38] the contact angle was measured by the sessile drop method at ambient pressure and temperature, with the distilled water and the coal sample as a liquid phase and a solid phase, respectively. The specific testing procedure was as follows: First, 0.2 g of the coal powder was weighed and poured into a mold. Then, it was pressed for 1 min with a DF-4B tablet machine at 15 MPa to obtain a coal slice with a diameter of 13 mm and thickness of 2 mm. Second, distilled water was injected into the syringe, and one drop of water (about 4 μL) was titrated onto the surface of the coal slice, thus the coal−water contact angle was formed on the surface. Then, the value of the contact angle could be automatically reported by the instrument. Three surfactants were dissolved in the distilled water with a concentration of 0.1 wt %, and the coal powder was soaked into the prepared solution for 24 h for treatment, and then pressed into a slice by the abovementioned method and dried for 72 h at 50 °C. Finally, the contact angle between the dry coal slice and distilled water was measured. The schematic diagram of the testing instruments and process is presented in Figure 3.

2.2.2. Infrared Spectrum Analysis Method. The molecular structure information of coal can be obtained from the infrared spectrum of the sample. Each functional group has the corresponding characteristic absorption peak, which reflects the vibration form of each group in the molecule. Because the coal structure is a heterogeneous mixture composed of multiple functional groups, the phenomenon of multipeak superposition may appear in the infrared spectrum curve. Thus, PeakFit software can be used to fit the absorption peaks of functional groups in the original infrared spectrum curve. For the absorption peaks in the same spectrum and the wavenumber range, the content of functional groups can be represented by the percentage of the peak area.[21,39]

2.2.3. Analysis Methods for Main Influencing Factors of Coal Wettability and the Treatment Effect. Since many factors affect coal wettability, different factors may correlate with each other, and the dimensions of each factor are different. Therefore, the relationship between the influencing factors and contact angle cannot be directly obtained. In this study, the grey system theory was applied to establish a model to eliminate the original data dimension, and then MATLAB software was used to run the model to investigate the main factors affecting the coal wettability and the main factors affecting the treatment effect of surfactants on coal wettability. The model establishment and calculation process are attached in the Appendix 1.

3. RESULTS

3.1. Basic Physical Parameters of Coal Samples.
Table 2 shows the results of proximate analysis and the contact angle of coal samples. As can be seen, the average maximum reflectance of vitrinite (R_o) ranges from 0.63 to 2.69%. With the increase in R_o, the metamorphic degree of coal increases. The

Table 4. Fitting Results of the Hydroxyl Group

sample	area	wavenumber (cm^{-1})	percentage of peak area (%)	functional group[a]
LJB	0.407	3038	3.36	OH···N
LJB	0.917	3246	7.58	ring hydroxyl
LJB	1.92	3367	15.87	OH···O
LJB	1.96	3483	16.20	OH···OH
LJB	1.477	3544	12.20	OH···π
LJB	0.931	3616	7.69	free hydroxyl
PN	0.384	3034	10.94	OH···N
PN	0.325	3242	9.27	ring hydroxyl
PN	0.448	3372	12.75	OH···O
PN	0.427	3492	12.16	OH···OH
PN	0.411	3557	11.71	OH···π
PN	0.439	3629	12.49	free hydroxyl
ZL	0.342	3040	9.38	OH···N
ZL	0.28	3249	7.68	ring hydroxyl
ZL	0.443	3353	12.15	OH···O
ZL	0.531	3446	14.56	OH···OH
ZL	0.366	3534	10.04	OH···π
ZL	0.137	3593	3.76	free hydroxyl
XK	2.336	3099	5.41	OH···N
XK	4.680	3258	10.84	ring hydroxyl
XK	9.335	3412	21.62	OH···O
XK	8.777	3502	20.33	OH···π
XK	7.597	3621	17.59	free hydroxyl
YG	1.375	3042	7.02	OH···N
YG	2.004	3197	10.23	ring hydroxyl
YG	4.787	3383	24.43	OH···O
YG	3.889	3460	19.85	OH···OH
YG	2.742	3538	14.00	OH···π
YG	1.703	3633	8.69	free hydroxyl
FC	1.014	3076	3.70	OH···N
FC	3.680	3262	13.44	ring hydroxyl
FC	5.037	3350	18.40	OH···O
FC	6.553	3426	23.94	OH···OH
FC	5.151	3507	18.82	OH···π
FC	1.186	3648	4.33	free hydroxyl

[a]Based on refs 21, 40, 47.

metamorphic degree of LJB, YG, PN, ZL, FC, and XK decreases successively. According to the Chinese national standard GB/T 5751−2009, the category of coal samples was classified. The content of moisture (M_{ad}), ash (A_{ad}), volatile matter (V_{daf}), and fixed carbon (FC_{ad}) are in the ranges of 0.89−10.62, 4.42−34.52, 8.44−44.47, and 41.09−76.22%, respectively. The range of coal−water contact angle of the original coal samples is 16.25−85.31°. After the coal was treated by APG and SDBS, the ranges of contact angle are 8.66−34.55 and 8.25−26.34° respectively, and the contact angle of all coal samples decreases significantly, indicating that the coal wettability was improved. Moreover, the contact angles of the coal samples treated with SDBS are smaller than those treated by APG, suggesting a better effect of SDBS than APG. However, after the treatment of PAM, the contact angles of coal samples ranged from 44.24 to 100.32°, and except for that of ZL and FC, which only decreased by 0.01 and 5.78°, respectively, the contact angles of all other coal samples increased, indicating that the PAM can weaken the coal wettability. Table 3 shows the contact angle of the coal samples. Figure 4 shows that with the increase in the metamorphic degree, the contact angle first increases and then decreases, which indicates that the coal wettability shows a high−low−high
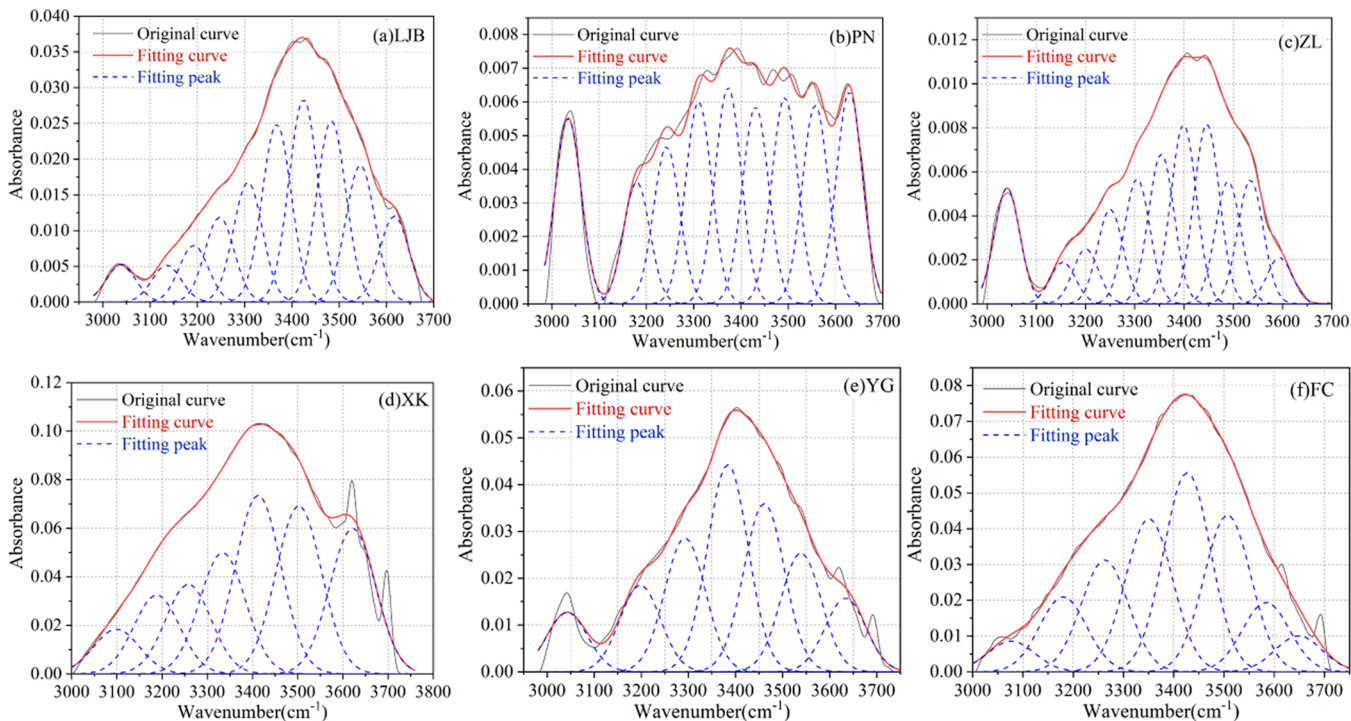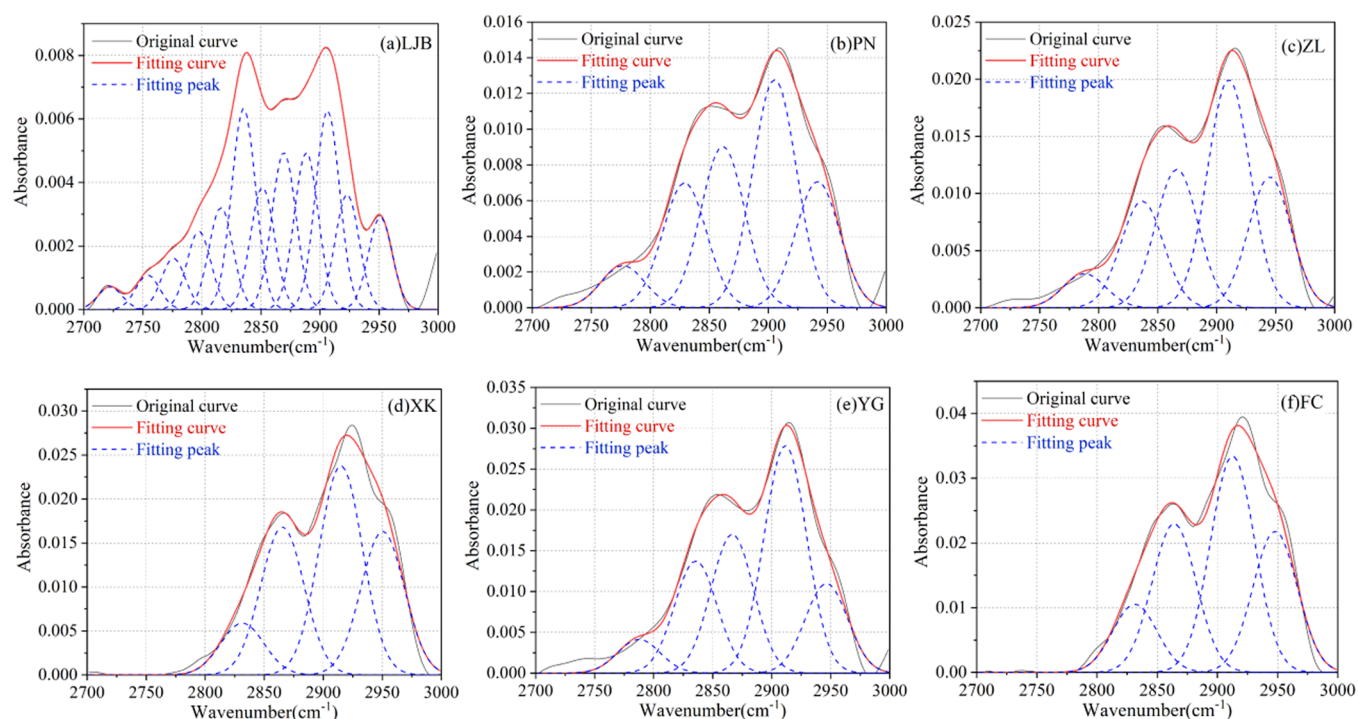
Figure 7. Fitting results of the infrared spectrum for 2700−3000 cm^{-1}. (a) LJB. (b) PN. (c) ZL. (d) XK. (e) YG. (f) FC.

trend with the increase in the metamorphic degree and is similar to Wang's[19] conclusion. As the coal rank increased from long flame coal to gas coal, the contact angle increased sharply, thus the coal wettability heavily deteriorated; when the coal rank increased from gas coal to anthracite, the contact angle showed an obvious downward reduction, correspondingly the coal wettability significantly improved. The wettability of long flame coal is the best and that of gas coal is the weakest.

3.2. Results of Infrared Spectrum Analysis. To compare the infrared spectra of each coal sample, the original infrared spectrum data was inputted into OMNIC software, and the infrared spectrum of coal was obtained, as shown in Figure 5. The range and distribution of peaks of each coal sample are almost the same, while the intensity of absorption peaks is different, indicating the different content of functional groups. According to previous studies, the vibration ranges of hydroxyl, aliphatic, oxygen-containing functional groups, and aromatic structures are 3000−3700, 2800−3000, 1000−1800, and 700−900 cm^{-1}, respectively.[21,40−46] To obtain the content of functional groups, PeakFit software was used to fit the original spectral curves in these four ranges (the shadow area in Figure 5). It should be noted that due to the interaction between functional groups, the wavenumber position of functional groups may have deviated.

3.2.1. Fitting Results of the Hydroxyl Group. Figure 6 shows the fitting results in the range of 3000−3700 cm^{-1}, and the position and the area of the hydroxyl absorption peak are given in Table 4. After the fitting of the original infrared spectrum, six kinds of hydroxyl functional groups were found: OH···N, ring hydroxyl, OH···O, OH···OH, OH···π, and free hydroxyl, and their characteristic peaks appear near the wavenumbers of 3048, 3226, 3387, 3467, 3526, and 3600 cm^{-1}, respectively.[21] Among them, the absorption peak of free hydroxyl is caused by the absorption of moisture in the air by coal samples during the test, and the percentage of the peak area is the percentage of the area of a functional group in areas of all functional

groups in the same wavenumber range. As presented in Table 4, all coal samples contain OH···N, ring hydroxyl, OH···O, OH···π, and OH···OH, except that OH···OH was not detected in the XK coal sample.

3.2.2. Fitting Results of the Aliphatic Functional Groups. Aliphatic functional groups are the functional groups that generate methane during coal pyrolysis. The fitting results in the range of 2700−3000 cm^{-1} are shown in Figure 7 and Table 5, which indicated that there are five kinds of absorption peaks formed by aliphatic functional groups: the absorption peak near 2832 cm^{-1} is caused by −CH stretching vibration, the absorption peaks near 2856 and 2895 cm^{-1} are caused by −CH$_2$ and −CH$_3$ symmetric stretching vibrations, respectively, and the absorption peaks near 2921 and 2953 cm^{-1} are caused by the asymmetric stretching vibrations of −CH$_2$ and −CH$_3$, respectively.[21,47] The fitting results indicate that all coal samples contain −CH, −CH$_2$, and −CH$_3$ aliphatic functional groups.

3.2.3. Fitting Results of the Oxygen-Containing Functional Groups. The fitting results in the range of 900−1800 cm^{-1} are shown in Figure 8 and Table 6, and there are five kinds of absorption peaks formed by oxygen-containing functional groups: the absorption peaks near 1010 and 1032 cm^{-1} are induced by the Si−O−Si antisymmetric stretching vibration, the absorption peaks near 1095 cm^{-1} are induced by the C−O−C stretching vibration, the absorption peaks near 1228, 1171, and 1115 cm^{-1} are induced by the C−O tensile vibration, the absorption peaks near 1299 cm^{-1} are induced by the N=O symmetric stretching vibration, and the absorption peaks near 1678 cm^{-1} are induced by the C=O tensile vibration.[21,47]

3.2.4. Fitting Results of the Aromatic Functional Groups. The fitting results in the range of 700−900 cm^{-1} are shown in Figure 9 and Table 7, which shows that there are four kinds of absorption peaks formed by aromatic functional groups: the absorption peaks near 754, 792, 823, and 860 cm^{-1} are formed by methylbenzene, 1,2-dimethylbenzene, 1,3-dimethylbenzene, and 1,4-dimethylbenzene, respectively.[21,47]

4. DISCUSSION

4.1. Effect of Surfactants on Coal Wettability. As can be seen in Table 1, after the samples were treated by APG and SDBS, the contact angles of all six coal samples decreased by 15−77 and 38−90%, respectively; while after being treated by PAM, the contact angles of coal samples increased by 18−72%, except for that of ZL and FC, which only decreased by 0.01 and 7%, respectively. Therefore, APG and SDBS can be used to improve the coal wettability, while PAM can weaken the coal wettability. As can be seen from Figure 10, SDBS is the most effective surfactant to decrease the contact angle and improve the coal wettability.

4.2. Main Influencing Factors of Coal Wettability. According to previous studies, coal wettability can be affected by the composition and chemical functional groups such as oxygen-containing functional groups, aliphatic chains, and aromatic hydrocarbon.[35,48] Some scholars reported that hydroxyl, quartz, moisture, and ash in coal are hydrophilic factors, while aliphatic chain, aromatic hydrocarbon, volatile, and fixed carbon are hydrophobic factors.[34,36,49] In this study, the main factors influencing coal wettability were calculated based on the grey relational analysis model. The content of moisture, ash, volatile, fixed carbon, functional groups, and the contact angle was input into MATLAB and the influence degree of these factors on coal wettability was obtained. The content of hydroxyl is the total content of OH⋯N, ring hydroxyl, OH⋯O, OH⋯π, and OH⋯OH, while the contact angle refers to the value before coal samples' treatment. The calculation process is attached in Appendixes 1.1 and 2.1.

Table 8 shows the relational degree (r_i) of each influencing factor and the contact angle obtained by MATLAB, where r_1, r_2, r_3, r_2, r_4, r_5, r_6, r_7, r_8, r_9, r_{10}, r_{11}, r_{12}, and r_{13} are the relational degrees of −CH, −CH$_2$, −CH$_3$, methylbenzene, 1,2-dimethylbenzene, 1,3-dimethylbenzene, 1,4-dimethylbenzene, V_{daf}, FC_{ad}, M_{ad}, A_{ad}, hydroxyl, and Si−O−Si with the contact angle, respectively. As presented in Table 7, r_7, r_2, r_{10}, r_{11}, r_3, r_{13}, r_{12}, r_8, r_5, r_1, r_4, r_9, and r_6 decrease successively, which indicates that the influence of 1,4-dimethylbenzene, −CH$_2$, M_{ad}, A_{ad}, −CH$_3$, Si−O−Si, hydroxyl, V_{daf}, 1,2-dimethylbenzene, −CH, methylbenzene, FC_{ad}, and 1,3-dimethylbenzene on coal wettability decreases in order. Among which, M_{ad}, A_{ad}, hydroxyl, and Si−O−Si are the hydrophilic factors and −CH$_2$, 1,4-dimethylbenzene, −CH$_3$, V_{daf}, 1,2-dimethylbenzene, methylbenzene, −CH, FC_{ad}, and 1,3-dimethylbenzene are the hydrophobic factors. Therefore, it is concluded that M_{ad} is the main hydrophilic factor of coal, and 1,4-dimethylbenzene is the main hydrophobic factor of coal.

4.3. Main Factors Affecting the Treatment Effect of the Surfactant. To obtain the main factors affecting the treatment effect of three surfactants on coal wettability, the dominance analysis method was applied. Specific related parameters and calculation programs are attached in Appendixes 1.2 and 2.2.

The incidence matrix (R) of influencing factors and contact angle was obtained by MATLAB

Table 5. Fitting Results of the Aliphatic Functional Group

sample	area	wavenumber (cm^{-1})	percentage of peak area (%)	functional group[a]
LJB	0.161	2835	15.08	−CH stretching vibration
LJB	0.098	2851	9.16	−CH$_2$ symmetric stretching vibration
LJB	0.126	2888	11.77	−CH$_3$ symmetric stretching vibration
LJB	0.092	2922	8.63	−CH$_2$ asymmetric stretching vibration
LJB	0.074	2951	6.93	−CH$_3$ asymmetric stretching vibration
PN	0.326	2829	18.29	−CH stretching vibration
PN	0.421	2861	23.62	−CH$_2$ symmetric stretching vibration
PN	0.595	2905	33.42	−CH$_3$ symmetric stretching vibration
PN	0.329	2941	18.49	−CH$_3$ asymmetric stretching vibration
ZL	0.422	2836	16.73	−CH stretching vibration
ZL	0.547	2866	21.69	−CH$_2$ symmetric stretching vibration
ZL	0.901	2910	35.73	−CH$_2$ asymmetric stretching vibration
ZL	0.517	2944	20.50	−CH$_3$ asymmetric stretching vibration
XK	0.272	2831	9.40	−CH stretching vibration
XK	0.775	2865	26.79	−CH$_2$ symmetric stretching vibration
XK	1.094	2914	37.82	−CH$_2$ asymmetric stretching vibration
XK	0.752	2950	25.99	−CH$_3$ asymmetric stretching vibration
YG	0.620	2835	18.64	−CH stretching vibration
YG	0.767	2866	23.06	−CH$_2$ symmetric stretching vibration
YG	1.256	2911	37.79	−CH$_2$ asymmetric stretching vibration
YG	0.495	2946	14.88	−CH$_3$ asymmetric stretching vibration
FC	0.486	2831	11.88	−CH stretching vibration
FC	1.058	2864	25.88	−CH$_2$ symmetric stretching vibration
FC	1.539	2912	37.65	−CH$_2$ asymmetric stretching vibration
FC	1.005	2947	24.58	−CH$_3$ asymmetric stretching vibration

[a]Based on refs 21, 47.

In the abovementioned R matrix, the elements in the first to third rows represent the relational degree between each factor and the contact angle of the coal samples treated by APG, SDBS, and PAM, respectively. As listed in the R matrix, the elements in the third row are almost the largest, indicating that the physicochemical properties of coal affected the treatment effect of PAM on coal wettability the most. In the first row, $r_{1,4} = 0.8316$ is the largest, indicating that aromatic methylbenzene has

$$R = \begin{bmatrix} 0.8281 & 0.7294 & 0.7409 & 0.8316 & 0.8270 & 0.6944 & 0.8217 & 0.6921 & 0.7958 & 0.6427 & 0.7151 & 0.8114 & 0.6961 \\ 0.8538 & 0.6681 & 0.8051 & 0.8402 & 0.8464 & 0.7344 & 0.8203 & 0.6466 & 0.8352 & 0.7017 & 0.7727 & 0.8597 & 0.7480 \\ 0.8889 & 0.6450 & 0.8497 & 0.8961 & 0.9016 & 0.7398 & 0.8680 & 0.7326 & 0.8500 & 0.6957 & 0.7863 & 0.9077 & 0.7505 \end{bmatrix}$$
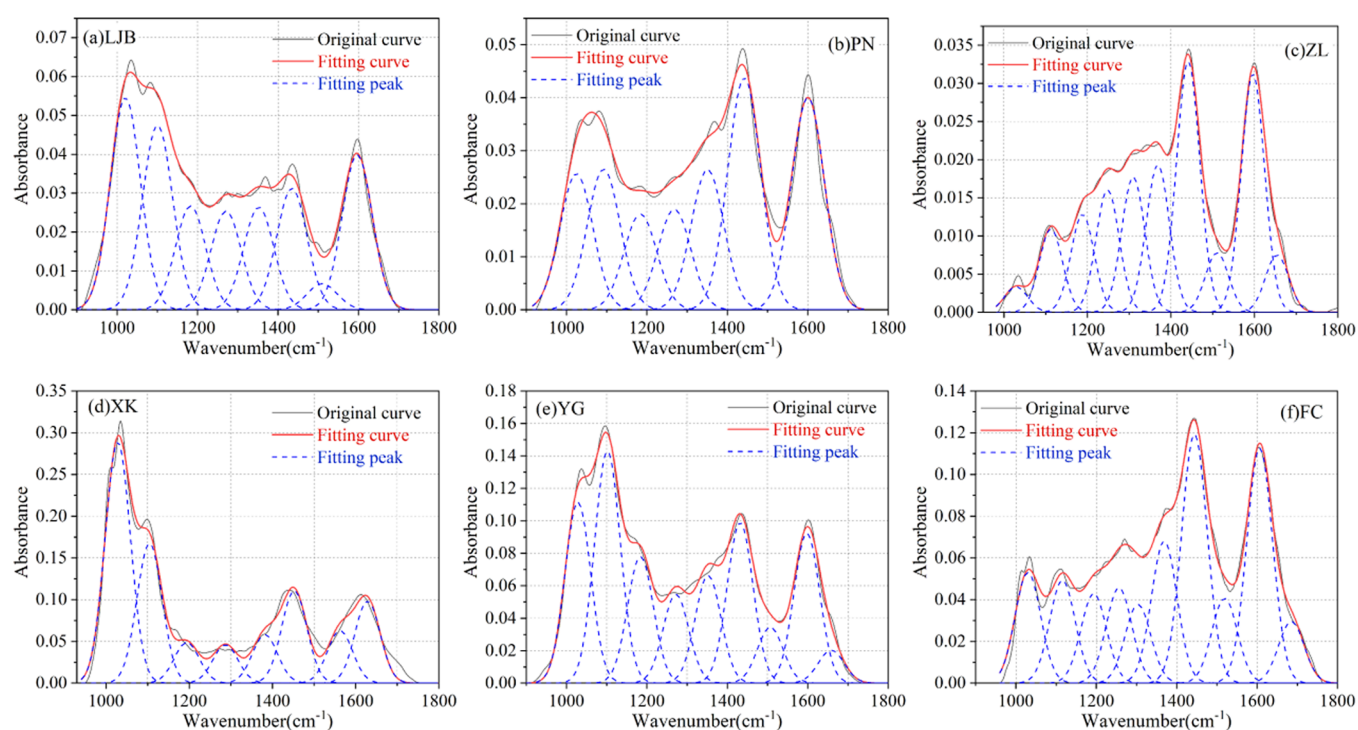
Figure 8. Fitting results of the infrared spectrum for 900−1800 cm^{-1}. (a) LJB. (b) PN. (c) ZL. (d) XK. (e) YG. (f) FC.

the greatest influence on the treatment effect of APG. In the second row, $r_{2,12}$ = 0.8597 is the largest, indicating that the hydroxyl content in coal was the main factor affecting the treatment effect of SDBS. In the third row, $r_{3,12}$ = 0.9077 is the largest, indicating that the hydroxyl group has the greatest influence on the treatment effect of PAM. Since SDBS is the most effective surfactant to improve the coal wettability (see Section 4.1) and the influence of hydroxyl, −CH, 1,2-dimethylbenzene, methylbenzene, FC$_{ad}$, 1,4-dimethylbenzene, −CH$_3$, A_{ad}, Si−O−Si, 1,3-dimethylbenzene, M_{ad}, −CH$_2$, and V_{daf} on its treatment effect decrease successively, it is concluded that an SDBS solution can be prepared based on the content of hydroxyl in coal. For coal with a low hydroxyl content, a higher concentration SDBS solution may be needed. In the process of water injection, the coal wettability can be improved by adding SDBS into the water, and then the efficiency of droplet capture of treated coal dust can be enhanced when spraying.

4.4. Implications for Field Application. In the fully mechanized coal mining face, the concentration of coal dust can reach up to 1000 mg/cm^3. Due to the poor wettability of coal dust, the dedusting efficiency of water spray is not ideal.[7−9] In this study, surfactants were used to treat the coal to improve the coal wettability so as to improve the wet dedusting efficiency. In the process of coal seam water injection, the coal wettability can be improved by adding a suitable surfactant into water. After that, when applying the spray dedusting technology, the floating coal dust with modified wettability and produced during the coal mining process can be more efficiently captured by water. Figure 11 shows the schematic diagram of dust suppression. Figure 12 shows the schematic of field implementation for future on-site operation. First, the surfactant solution was injected into the coal seam and high-pressure water was used to keep the pressure of the water injection borehole for 15 days.[14] Then, the coal mining machine was used to mine the coal treated with the surfactant and the nozzle was opened on the hydraulic support to reduce coal dust. This paper

Table 6. Fitting Results of the Oxygen-Containing Functional Group

sample	area	wavenumber (cm^{-1})	percentage of peak area (%)	functional group[a]
LJB	5.143	1020	21.12	Si−O−Si antisymmetric stretching vibration
LJB	4.471	1100	18.36	C−O−C stretching vibration
LJB	2.519	1182	10.35	C−O tensile vibration
LJB	2.393	1270	9.83	N=O symmetric stretching vibration
PN	2.632	1024	12.87	Si−O−Si antisymmetric stretching vibration
PN	2.723	1092	13.32	C−O−C stretching vibration
PN	1.851	1183	9.05	C−O tensile vibration
PN	1.943	1268	9.50	N=O symmetric stretching vibration
ZL	0.233	1028	2.10	Si−O−Si antisymmetric stretching vibration
ZL	0.761	1112	16.9	C−O tensile vibration
ZL	1.117	1248		
ZL	1.232	1309	11.08	N=O symmetric stretching vibration
XK	22.004	1028	32.80	Si−O−Si antisymmetric stretching vibration
XK	12.751	1104	19.01	C−O−C stretching vibration
XK	3.714	1193	5.54	C−O tensile vibration
XK	3.506	1287	5.23	N=O symmetric stretching vibration
YG	8.967	1028	15.92	Si−O−Si antisymmetric stretching vibration
YG	11.507	1101	20.43	C−O−C stretching vibration
YG	6.282	1183	11.15	C−O tensile vibration
YG	4.409	1272	7.83	N=O symmetric stretching vibration
YG	1.640	1658	2.91	C=O tensile vibration

Table 6. continued

sample	area	wavenumber (cm^{-1})	percentage of peak area (%)	functional group[a]
FC	4.252	1029	8.81	Si—O—Si antisymmetric stretching vibration
FC	3.944	1115	15.28	C—O tensile vibration
FC	3.436	1193		
FC	3.025	1303	6.26	N=O symmetric stretching vibration
FC	2.370	1685	4.91	C=O tensile vibration

[a]Based on refs 21, 47.

provides an efficient way to select the most effective surfactant among different surfactants to improve the coal wettability and to investigate the main factors affecting the modification effect of surfactants. Considering the influence of coal properties on the modification effect of the surfactant, a suitable surfactant can be selected to treat coal and then to improve the wet dedusting efficiency.

5. CONCLUSIONS

To investigate the main influencing physicochemical properties of coal on the coal wettability and the treatment effect of the surfactant, the coal−water contact angle was used as an index to evaluate the coal wettability, and three surfactants were applied to treat the coal. The relationship between basic physical properties, the chemical functional group structure of coal, and the contact angle was investigated by grey system theory. The main conclusions are as follows:

(1) The coal wettability shows a high−low−high trend with the increase in the metamorphic degree. The wettability of long flame coal is the strongest and that of gas coal is the weakest. For the coal samples treated by APG and SDBS, the contact angle decreased by 15−77 and 38−90%, respectively. However, for the coal samples treated

by PAM, except for the contact angles of ZL and FC, which only decreased by 0.01 and 7%, respectively, the contact angles of other samples increased by 18−72%. Thus, APG and SDBS can improve the coal wettability and PAM can weaken the coal wettability. The anionic surfactant SDBS is the most effective surfactant to improve the coal wettability, which can be used to improve wet dedusting efficiency such as coal seam water injection and water spray.

(2) The results of the grey relational analysis show that the relational degree of 1,4-dimethylbenzene, −CH$_2$, moisture, ash, −CH$_3$, Si−O−Si, hydroxyl, volatile matter, 1,2-dimethylbenzene, −CH, methylbenzene, fixed carbon, and 1,3-dimethylbenzene with the contact angle decreases in order. Moisture is the main hydrophilic factor of coal and 1,4-dimethylbenzene is the main hydrophobic factor of coal.

(3) The main factors affecting the treatment effect of APG, SDBS, and PAM are the aromatic methylbenzene, hydroxyl, and hydroxyl content of coal, respectively. Among these three surfactants, the treatment effect of PAM on coal wettability was affected by the physicochemical properties of coal the most. The most effective surfactant SDBS solution can be used to improve the coal wettability and prepared based on the hydroxyl content of coal. For coal with a low hydroxyl content, a higher concentration SDBS solution could be needed.

■ APPENDIX 1. CALCULATION PROCESS OF GREY SYSTEM THEORY

Grey system theory is a method that can be used to investigate the mathematical relationship between factors based on the characteristic data of the grey system and the explicit and implicit information in the data.[50] In this study, two methods of grey system theory, relational analysis and dominance analysis, were used to calculate the main factors affecting the
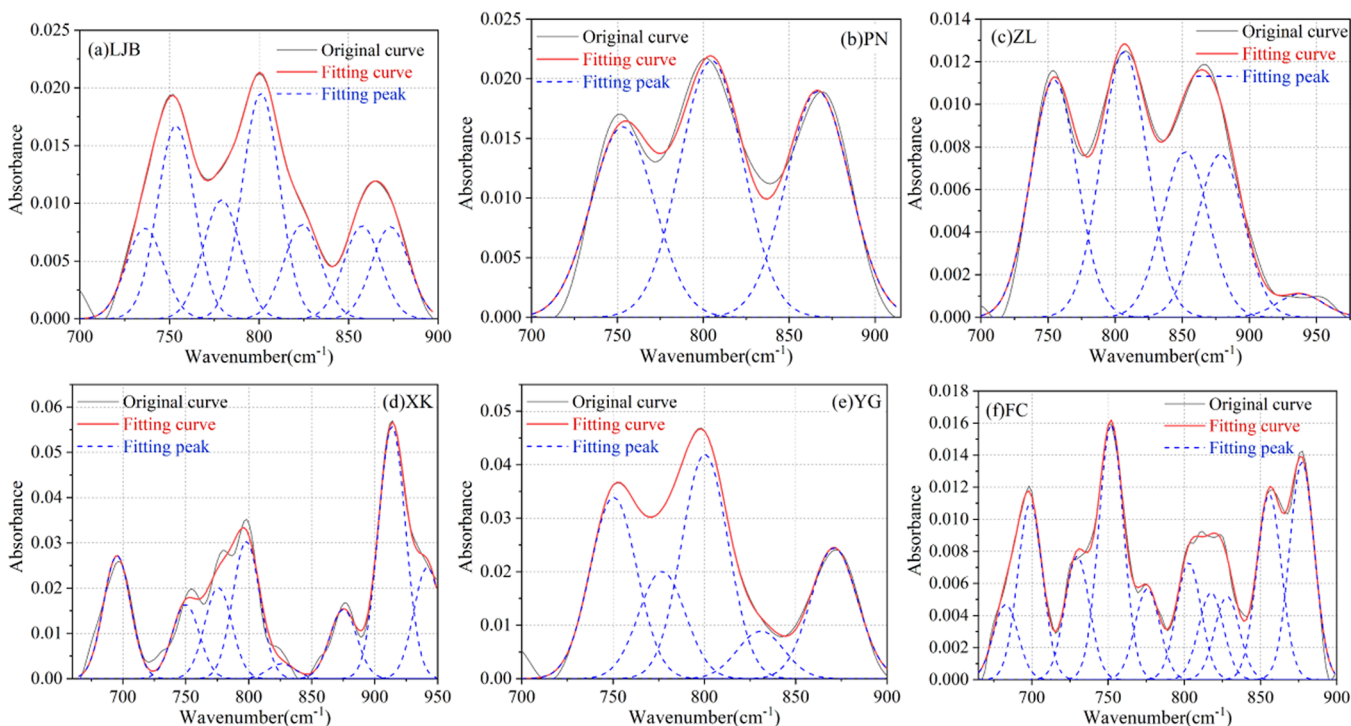

Figure 9. Fitting results of the infrared spectrum for 700−900 cm^{-1}. (a) LJB. (b) PN. (c) ZL. (d) XK. (e) YG. (f) FC.

Table 7. Fitting Results of the Aromatic Functional Group

| sample	area	wavenumber (cm^{-1})	percentage of peak area (%)	functional group[a]
LJB	0.434	753	21.29	methylbenzene
LJB	0.507	801	24.88	1,2-dimethylbenzene
LJB	0.212	824	10.41	1,3-dimethylbenzene
LJB	0.208	857	10.23	1,4-dimethylbenzene
PN	0.74	753	28.32	methylbenzene
PN	0.996	804	38.12	1,2-dimethylbenzene
PN	0.877	866	33.56	1,4-dimethylbenzene
ZL	0.482	754	27.70	methylbenzene
ZL	0.54	806	31.03	1,2-dimethylbenzene
ZL	0.34	852	19.54	1,4-dimethylbenzene
XK	0.432	750	8.51	methylbenzene
XK	0.798	798	15.73	1,2-dimethylbenzene
XK	0.087	826	1.71	1,3-dimethylbenzene
XK	0.404	875	7.96	1,4-dimethylbenzene
YG	1.085	750	26.23	methylbenzene
YG	1.342	800	32.44	1,2-dimethylbenzene
YG	0.285	830	6.89	1,3-dimethylbenzene
YG	0.782	870	18.91	1,4-dimethylbenzene
FC	0.323	751	18.07	methylbenzene
FC	0.148	802	8.29	1,2-dimethylbenzene
FC	0.105	828	5.90	1,3-dimethylbenzene
FC	0.235	855	13.14	1,4-dimethylbenzene

[a]Based on refs 21, 47.
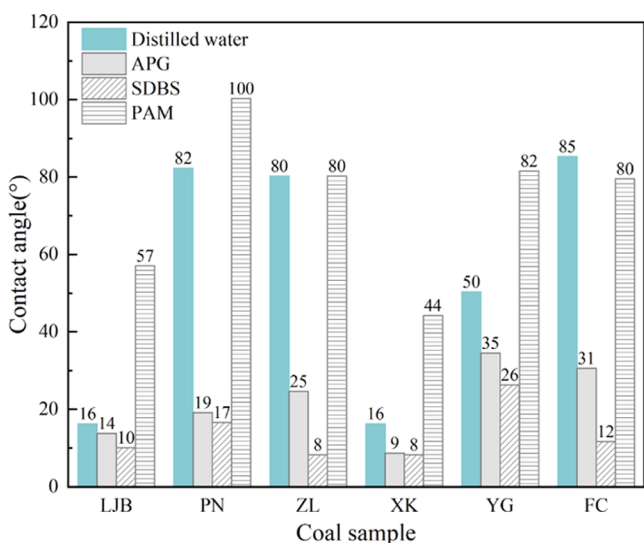
Figure 10. Contact angle of coal samples before and after treatment.

coal wettability and the treatment effect of different surfactants. The specific calculation process is as follows:

Appendix 1.1. Grey Relational Analysis Model
Grey relational analysis is a method that can measure the degree of correlation between factors based on the similarity or dissimilarity of the development trend of factors. The process of grey relational analysis in this study is as follows:

(1). Determine the Reference Sequence.

$$x_0 = \{x_0(k)|k = 1, 2, ..., n\} = (x_0(1), x_0(2), ..., x_0(n))$$

(1)

where k is the number of coal samples, $n = 1, 2, ..., 6$, and the reference sequence is the contact angle of untreated coal samples.

(2). Determine the Comparison Sequence.

$$x_i = \{x_i(k)|k = 1, 2, ..., n\} = (x_i(1), x_i(2), ..., x_i(n))$$
$$, i = 1, 2, ..., 13$$

(2)

where x_i is the influencing factor of contact angle, and the parameters represented by x_i are listed in Table 9.

(3). Initialization of the Sequence. To eliminate the dimension of the sequence, the sequence $x = (x(1), x(2), ..., x(n))$ was initialized by eq 3

$$\bar{x} = \left(1, \frac{x(2)}{x(1)}, ..., \frac{x(n)}{x(1)}\right)$$

(3)

where $\bar{x}$ is the initialization sequence of the original sequence.

However, because the contact angle decreases with the increase in hydroxyl, quartz, moisture, and ash content,[51] eq 4 was used to initialize them

$$x_i = \left(1, \frac{x_i(1)}{x_i(2)}, \frac{x_i(1)}{x_i(3)}, ..., \frac{x_i(1)}{x_i(6)}\right), \quad i = 10, 11, 12, 13$$

(4)

(4). Calculate the Grey Relational Coefficient.

$$\xi_i(k) = \frac{\min_s \min_t |x_0(t) - x_s(t)| + \rho \max_s \max_t |x_0(t) - x_s(t)|}{|x_0(k) - x_i(k)| + \rho \max_s \max_t |x_0(t) - x_s(t)|}$$

(5)

where $\xi_i(k)$ is the relational coefficient of the comparison sequence x_i and the reference sequence x_0 when the coal sample number is k. It is an index to characterize the relational degree between the comparison sequence and the reference sequence; $\rho \in [0,1]$, is the resolution coefficient, and generally $\rho = 0.5$.[52,53] $\min_s \min_t |x_0(t) - x_s(t)|$ and $\max_s \max_t |x_0(t) - x_s(t)|$ are the minimum difference between two levels and the maximum difference between two levels, respectively.

(5) Since each coal sample in eq 5 has a relational coefficient, the information is scattered and cannot be directly compared, it is necessary to calculate the grey relational degree

$$r_i = \frac{1}{n} \sum_{k=1}^{n} \xi_i(k)$$

(6)

where r_i is the relational degree between the influencing factors and the contact angle. The larger the value of the relational degree, the better the relationship between the influencing factors and contact angle.

Based on the grey relational analysis model and the parameters listed in Table 9, through the calculation of the MATLAB program (see Appendix 2.1), the relational degree can be obtained, as presented in Table 8.

Appendix 1.2. Dominance Analysis
When there is more than one reference sequence, the dominance analysis method needs to be used to calculate the relational degree. The contact angles of coal samples under three different conditions were measured, thus there are 3 reference sequences y_1, y_2, y_3, and 13 comparison sequences $x_1, x_2, ..., x_{13}$. The parameters represented by each sequence are listed in Table 10. Defining $r_{i,j}$ as the relational degree of the comparison sequence x_j to the reference sequence y_i, then the incidence matrix $R = (r_{i,j})_{3 \times 13}$ could be constructed. According to the elements in the matrix R, the main

Table 8. Relational Degree (r_i) of Each Influencing Factor and the Contact Angle

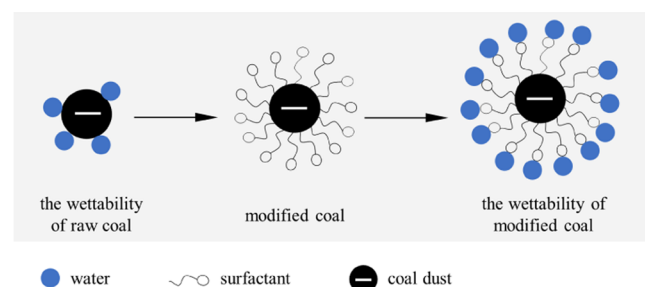| r_1	r_2	r_3	r_4	r_5	r_6	r_7	r_8	r_9	r_{10}	r_{11}	r_{12}	r_{13}
0.6027	0.6654	0.6195	0.5962	0.6059	0.5496	0.6722	0.6067	0.5890	0.6626	0.6348	0.6069	0.6173

Figure 11. Schematic diagram of water capturing the coal dust.

influencing factors of the contact angle under different conditions can be analyzed, and the main factors affecting the treatment effect of three surfactants on coal can be obtained. When a row element is larger than other row elements, the parent element corresponding to this row is the dominant parent element. When a column element is larger than other column elements, the corresponding subfactor of this column is the dominant subfactor. The data in Table 10 were input into MATLAB and the MATLAB program was run for dominance analysis (see Appendix 2.2), by which the matrix R could be obtained.
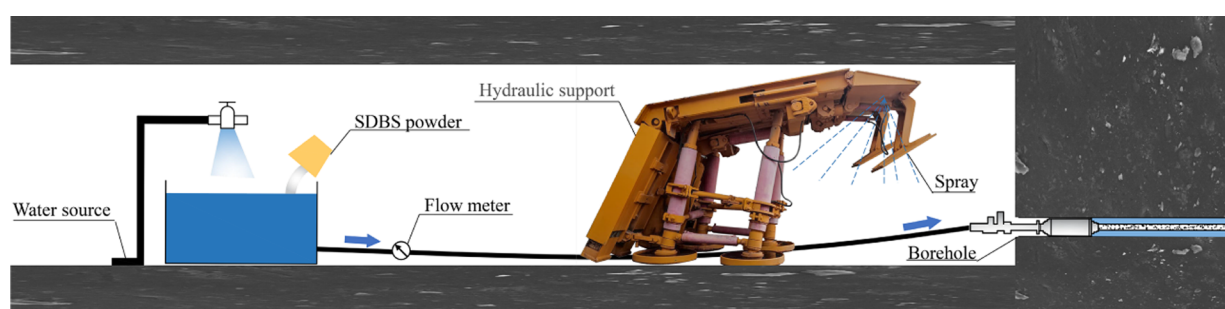

Figure 12. Schematic of the field operation process.

Table 9. Parameters for Grey Relational Analysis

coal sample	LJB	PN	ZL	XK	YG	FC
contact angle x_0	16.26	82.31	80.26	16.25	50.37	85.31
−CH x_1	15.08	18.29	16.73	9.4	18.64	11.88
−CH$_2$ x_2	17.79	23.62	57.42	64.61	60.85	63.53
−CH$_3$ x_3	18.7	51.91	20.5	25.99	14.88	24.58
methylbenzene x_4	21.29	28.32	27.7	8.51	26.23	18.07
1,2-dimethylbenzene x_5	24.88	38.12	31.03	15.73	32.44	8.29
1,3-dimethylbenzene x_6	10.41	0	0	1.71	6.89	5.9
1,4-dimethylbenzene x_7	10.23	33.56	19.54	7.96	18.91	13.14
V_{daf} x_8	8.44	16.25	20.38	44.47	11.98	35.36
FC_{ad} x_9	75.95	73.59	76.22	41.09	71.06	59.46
M_{ad} x_{10}	2.66	0.94	0.89	10.62	1.34	1.84
A_{ad} x_{11}	15.58	13.66	4.24	34.52	20.54	11.4
hydroxyl x_{12}	55.21	56.83	53.81	58.2	75.53	78.3
Si−O−Si x_{13}	21.12	12.87	2.1	32.8	15.92	8.81

Table 10. Parameters for Dominance Analysis

coal sample	LJB	PN	ZL	XK	YG	FC
contact angle (APG) y_1	13.79	19.11	24.59	8.66	34.55	30.58
contact angle (SDBS) y_2	10.12	16.63	8.29	8.25	26.34	11.65
contact angle (PAM) y_3	57.07	100.32	80.25	44.24	81.56	79.53
−CH x_1	15.08	18.29	16.73	9.4	18.64	11.88
−CH$_2$ x_2	17.79	23.62	57.42	64.61	60.85	63.53
−CH$_3$ x_3	18.7	51.91	20.5	25.99	14.88	24.58
methylbenzene x_4	21.29	28.32	27.7	8.51	26.23	18.07
1,2-dimethylbenzene x_5	24.88	38.12	31.03	15.73	32.44	8.29
1,3-dimethylbenzene x_6	10.41	0	0	1.71	6.89	5.9
1,4-dimethylbenzene x_7	10.23	33.56	19.54	7.96	18.91	13.14
V_{daf} x_8	8.44	16.25	20.38	44.47	11.98	35.36
FC_{ad} x_9	75.95	73.59	76.22	41.09	71.06	59.46

Table 10. continued

coal sample	LJB	PN	ZL	XK	YG	FC
$M_{ad}\ x_{10}$	2.66	0.94	0.89	10.62	1.34	1.84
$A_{ad}\ x_{11}$	15.58	13.66	4.24	34.52	20.54	11.4
hydroxyl x_{12}	55.21	56.83	53.81	58.2	75.53	78.3
Si−O−Si x_{13}	21.12	12.87	2.1	32.8	15.92	8.81

■ APPENDIX 2. MATLAB PROGRAM FOR CALCULATION

Appendix 2.1. MATLAB Program of Grey Relational Analysis

```
save x
  clc, clear
  load x
  for i=1:10
  x(i,:)=x(i,:)/x(i,1);
  end
  for i=11:14
  x(i,:)=x(i,1)./x(i,:);
  end
  data=x;
  n=size(data,1);
  ck=data(1,:);m1=size(ck,1);
  bj=data(2:n,:);m2=size(bj,1);
  for i=1:m1
  for j=1:m2
  t(j,:)=bj(j,:)-ck(i,:);
  end
  jc1=min(min(abs(t')));jc2=max(max(abs(t')));
  rho=0.5;
  ksi=(jc1+rho*jc2)./(abs(t)+rho*jc2);
  rt=sum(ksi')/size(ksi,2);
  r(i,:)=rt;
  end r
```

Appendix 2.1. MATLAB Program of dominance analysis

```
save data
  clc, clear
  load data
  n=size(data,1);
  for i=1:n
  data(i,:)=data(i,:)/data(i,1);
  end
  ck=data(14:n,:);m1=size(ck,1);
  bj=data(1:13,:);m2=size(bj,1);
  for i=1:m1
  for j=1:m2
  t(j,:)=bj(j,:)-ck(i,:);
  end
  jc1=min(min(abs(t')));jc2=max(max(abs(t')));
  rho=0.5;
  ksi=(jc1+rho*jc2)./(abs(t)+rho*jc2);
  rt=sum(ksi')/size(ksi,2);
  r(i,:)=rt;
  end r
```

■ AUTHOR INFORMATION

Corresponding Authors

Liang Wang − *Key Laboratory of Gas and Fire Control for Coal Mines, China University of Mining and Technology, Ministry of Education, Xuzhou 221116, China; School of Safety Engineering, China University of Mining and Technology, Xuzhou 221116, China;* ⓞ orcid.org/0000-0001-6815-9737; Phone: 86516 83590595; Email: wangliang@cumt.edu.cn

Jintuo Zhu − *Key Laboratory of Gas and Fire Control for Coal Mines, China University of Mining and Technology, Ministry of Education, Xuzhou 221116, China; School of Safety Engineering, China University of Mining and Technology, Xuzhou 221116, China;* Email: zhjtcumt@163.com

Authors

Xiaoxue Liao − *Key Laboratory of Gas and Fire Control for Coal Mines, China University of Mining and Technology, Ministry of Education, Xuzhou 221116, China; School of Safety Engineering, China University of Mining and Technology, Xuzhou 221116, China*

Bo Wang − *Key Laboratory of Gas and Fire Control for Coal Mines, China University of Mining and Technology, Ministry of Education, Xuzhou 221116, China; School of Safety Engineering, China University of Mining and Technology, Xuzhou 221116, China*

Peng Chu − *Key Laboratory of Gas and Fire Control for Coal Mines, China University of Mining and Technology, Ministry of Education, Xuzhou 221116, China; School of Safety Engineering, China University of Mining and Technology, Xuzhou 221116, China*

Zibin Zhu − *Key Laboratory of Gas and Fire Control for Coal Mines, China University of Mining and Technology, Ministry of Education, Xuzhou 221116, China; School of Safety Engineering, China University of Mining and Technology, Xuzhou 221116, China*

Siwen Zheng − *Key Laboratory of Gas and Fire Control for Coal Mines, China University of Mining and Technology, Ministry of Education, Xuzhou 221116, China; School of Safety Engineering, China University of Mining and Technology, Xuzhou 221116, China*

Complete contact information is available at:
https://pubs.acs.org/10.1021/acsomega.1c02205

Author Contributions

[§]Co-first author: X.L. and B.W. contributed equally to this work.

Notes

The authors declare no competing financial interest.

■ REFERENCES

(1) Cai, P.; Nie, W.; Chen, D.; Yang, S.; Liu, Z. Effect of air flowrate on pollutant dispersion pattern of coal dust particles at fully mechanized mining face based on numerical simulation. *Fuel* **2019**, *239*, 623−635.

(2) Gianoncelli, A.; Rizzardi, C.; Salomon, D.; Canzonieri, V.; Pascolo, L. Nano-imaging of environmental dust in human lung tissue by soft and hard X-ray fluorescence microscopy. *Spectrochim. Acta, Part B* **2018**, *147*, 71−78.

(3) Fang, X.; Yuan, L.; Jiang, B.; Zhu, W.; Ren, B.; Chen, M.; Mu, M.; Yu, G.; Li, P. Effect of water-fog particle size on dust fall efficiency of mechanized excavation face in coal mines. *J. Cleaner Prod.* **2020**, *254*, No. 120146.

(4) Chang, P.; Xu, G.; Chen, Y.; Ghosh, A.; Moridi, M. A. Improving coal powder wettability using electrolyte assisted surfactant solution. *Colloids Surf., A* **2021**, *613*, No. 126042.

(5) Bao, Q.; Liu, Y.; Li, C.; Jia, L.; Yan, J.; Yuan, M.; Zhou, W. Development and performance characterization of a hybrid dust suppressant based on sodium ligninsulfonate modification. *Starch-Stärke* **2021**, *73*, No. 2000207.

(6) Chang, P.; Zhao, Z.; Xu, G.; Ghosh, A.; Huang, J.; Yang, T. Evaluation of the coal dust suppression efficiency of different surfactants: A factorial experiment. *Colloids Surf., A* **2020**, *595*, No. 124686.

(7) Wang, J.; Zhou, G.; Wei, X.; Wang, S. Experimental characterization of multi-nozzle atomization interference for dust reduction between hydraulic supports at a fully mechanized coal mining face. *Environ. Sci. Pollut. Res.* **2019**, *26*, 10023−10036.

(8) Bao, Q.; Nie, W.; Liu, C.; Zhang, H.; Wang, H.; Jin, H.; Yan, J.; Liu, Q. The preparation of a novel hydrogel based on crosslinked polymers for suppressing coal dusts. *J. Cleaner Prod.* **2020**, *249*, No. 119343.

(9) Ji, H.; Peng, X.; Yao, J.; Mao, Y.; Hou, Y.; Sheng, Z. Insight into the influence of small organic molecules on the wettability of coal. *Fuel* **2021**, *294*, No. 120537.

(10) Lu, Y.; Li, H.; Lu, J. X.; Shi, S.; Wang, G.; Ye, Q.; Li, R.; Zhu, X. Clean up water blocking damage in coalbed methane reservoirs by microwave heating: Laboratory studies. *Process Saf. Environ. Prot.* **2020**, *138*, 292−299.

(11) Lyu, S.; Chen, X.; Shah, S.-M.; Wu, X. Experimental study of influence of natural surfactant soybean phospholipid on wettability of high-rank coal. *Fuel* **2019**, *239*, 1−12.

(12) Jia, L.; Li, K.; Zhou, J.; Yan, Z.; Wang, Y.; Mahlalela, B.-M. Experimental study on enhancing coal-bed methane production by wettability alteration to gas wetness. *Fuel* **2019**, *255*, No. 115860.

(13) Ni, G.; Li, Z.; Xie, H. The mechanism and relief method of the coal seam water blocking effect (WBE) based on the surfactants. *Powder Technol.* **2018**, *323*, 60−68.

(14) Li, J.; Li, K.; Shi, X.; Zhao, L.; Linghu, J. Application of gas wettability alteration to improve methane drainage performance: A case study. *Int. J. Min. Sci. Technol.* **2021**, *32*, 621−629.

(15) Shi, G.-Q.; Han, C.; Wang, Y.-m.; Wang, H.-T. Experimental study on synergistic wetting of a coal dust with dust suppressant compounded with noncationic surfactants and its mechanism analysis. *Powder Technol.* **2019**, *356*, 1077−1086.

(16) Han, W.; Zhou, G.; Zhang, Q.; Pan, H.; Liu, D. Experimental study on modification of physicochemical characteristics of acidified coal by surfactants and ionic liquids. *Fuel* **2020**, *266*, No. 116966.

(17) Zhang, H.; Nie, W.; Yan, J.; Bao, Q.; Wang, H.; Jin, H.; Peng, H.; Chen, D.; Liu, Z.; Liu, Q. Preparation and performance study of a novel polymeric spraying dust suppression agent with enhanced wetting and coagulation properties for coal mine. *Powder Technol.* **2020**, *364*, 901−914.

(18) Ni, G.; Wang, H.; Nie, B.; Wang, Y.; Dou, H.; Lu, S.; Wang, G. Research of wetting selectivity and wetting effect of imidazole ionic liquids on coal. *Fuel* **2021**, *286*, No. 119331.

(19) Wang, X.; Yuan, S.; Jiang, B. Experimental investigation of the wetting ability of surfactants to coals dust based on physical chemistry characteristics of the different coal samples. *Adv. Powder Technol.* **2019**, *30*, 1696−1708.

(20) Jiang, B.; Sun, Q.; Ni, G. Study on the wettability of a composite solution based on surface structures of coal. *ACS Omega* **2020**, *5*, 28341−28350.

(21) Ni, G.; Sun, Q.; Xue, M.; Wang, H.; Xu, Y.; Cheng, W.; Wang, G. Effect of NaCl-SDS compound solution on the wettability and functional groups of coal. *Fuel* **2019**, *257*, No. 116077.

(22) Zhou, Q.; Qin, B.; Ma, D.; Jiang, N. Novel technology for synergetic dust suppression using surfactant-magnetized water in underground coal mines. *Process Saf. Environ. Prot.* **2017**, *109*, 631−638.

(23) Sang, F.; Yan, S.; Wang, G.; Ma, Z.; Li, J.; Ju, S. The effect of microemulsion on coal wetting characteristics and physicochemical structure. *Colloid Interface Sci. Commun.* **2020**, *39*, No. 100335.

(24) Ma, Y.; Sun, J.; Ding, J.; Liu, Z. Synthesis and characterization of a penetrating and pre-wetting agent for coal seam water injection. *Powder Technol.* **2021**, *380*, 368−376.

(25) Yang, M.; Lu, Y.; Ge, Z.; Zhou, Z.; Chai, C.; Wang, H.; Zhang, L.; Bo, T. Viscoelastic surfactant fracturing fluids for use in coal seams: Effects of surfactant composition and formulation. *Chem. Eng. Sci.* **2020**, *215*, No. 115370.

(26) Wang, G.; Huang, T.; Yan, S.; Liu, X. Experimental study of the fracturing-wetting effect of VES fracturing fluid for the coal seam water injection. *J. Mol. Liq.* **2019**, *295*, No. 111715.

(27) Liu, C.; Sang, S.; Fan, X.; Zhang, K.; Song, F.; Cui, X.; Wang, H. Influences of pressures and temperatures on pore structures of different rank coals during CO_2 geological storage process. *Fuel* **2020**, *259*, No. 116273.

(28) Zheng, L.; Liu, Z.; Li, D.; Wang, H.; Zhang, Q. Micro-mechanism analysis of surfactant wetting of coal based on C-13 NMR experiments. *Acs Omega* **2021**, *6*, 1378−1390.

(29) Zhou, Q.; Xu, G.; Chen, Y.; Qin, B.; Zhao, Z.; Guo, C. The development of an optimized evaluation system for improving coal dust suppression efficiency using aqueous solution sprays. *Colloids Surf., A* **2020**, *602*, No. 125104.

(30) Ma, Y.; Wang, Y.; Zhang, Q. Experimental study for influence of surfactants chemical microstructures on wetting effect about coal dust in Tongchuan Mining Area. *J. Chem.* **2020**, *2020*, No. 4176186.

(31) Xu, C.; Wang, D.; Wang, H.; Ma, L.; Zhu, X.; Zhu, Y.; Zhang, Y.; Liu, F. Experimental investigation of coal dust wetting ability of anionic surfactants with different structures. *Process Saf. Environ. Prot.* **2019**, *121*, 69−76.

(32) Arif, M.; Jones, F.; Barifcani, A.; Iglauer, S. Influence of surface chemistry on interfacial properties of low to high rank coal seams. *Fuel* **2017**, *194*, 211−221.

(33) Arif, M.; Barifcani, A.; Lebedev, M.; Iglauer, S. CO_2-wettability of low to high rank coal seams: Implications for carbon sequestration and enhanced methane recovery. *Fuel* **2016**, *181*, 680−689.

(34) Hongchao, X.; Guanhua, H.; Jingna, X.; Weimin, C.; Meng, X.; Yuhang, X.; Hui, W.; Gang, W. The effect of SDS synergistic composite acidification on the chemical structure and wetting characteristics of coal. *Powder Technol.* **2020**, *367*, 253−265.

(35) Xu, C.; Wang, D.; Wang, H.; Xin, H.; Ma, L.; Zhu, X.; Zhang, Y.; Wang, Q. Effects of chemical properties of coal dust on its wettability. *Powder Technol.* **2017**, *318*, 33−39.

(36) Wang, H.; Zhang, L.; Wang, D.; He, X. Experimental investigation on the wettability of respirable coal dust based on infrared spectroscopy and contact angle analysis. *Adv. Powder Technol.* **2017**, *28*, 3130−3139.

(37) Semenova, S.-A.; Patrakov, Y.-F. Dependence of the water wettability of the surfaces of fossil coals on their structure and properties. *Solid Fuel Chem.* **2017**, *51*, 135−140.

(38) Shi, Q.; Qin, B.; Bi, Q.; Qu, B. Changes in the surface structure of coal caused by igneous intrusions and their effect on the wettability. *Energy Fuels* **2018**, *32*, 9371−9379.

(39) Weng, S.; Xu, Y. *Fourier Transform Infrared Spectroscopy*, 2nd ed.; Chemical Industry Press: Beijing, 2019; Vol. *478*, pp 224−231.

(40) Li, Q.; Lin, B.; Zhao, C.; Wu, W. Chemical structure analysis of coal char surface based on Fourier-transform infrared spectrometer. *Proc. Chin. Soc. Electr. Eng.* **2011**, *31*, 46−52.

(41) Zhao, J.; Deng, J.; Chen, L.; Wang, T.; Song, J.; Zhang, Y.; Shu, C.; Zeng, Q. Correlation analysis of the functional groups and exothermic characteristics of bituminous coal molecules during high-temperature oxidation. *Energy* **2019**, *181*, 136−147.

(42) Jingna, X.; Ni, G.; Hongchao, X.; Shang, L.; Qian, S.; Kai, D. The effect of adding surfactant to the treating acid on the chemical properties of an acid-treated coal. *Powder Technol.* **2019**, *356*, 263−272.

(43) He, X.; Liu, X.; Nie, B.; Song, D. FTIR and Raman spectroscopy characterization of functional groups in various rank coals. *Fuel* **2017**, *206*, 555−563.

(44) Ibarra, J.; Muoz, E.; Moliner, R. FTIR study of the evolution of coal structure during the coalification process. *Org. Geochem.* **1996**, *24*, 725−735.

(45) Jiang, J.; Yang, W.; Cheng, Y.; Liu, Z.; Zhang, Q.; Zhao, K. Molecular structure characterization of middle-high rank coal via XRD, Raman and FTIR spectroscopy: Implications for coalification. *Fuel* **2019**, *239*, 559−572.

(46) Zhang, L.; Hu, S.; Chen, Q.; Xiao, L.; Syed-Hassan, S.; Jiang, L.; Wang, Y.; Su, S.; Xiang, J. Molecular structure characterization of the tetrahydrofuran-microwave-extracted portions from three Chinese low-rank coals. *Fuel* **2017**, *189*, 178−185.

(47) Song, H.; Liu, G.; Zhang, J.; Wu, J. Pyrolysis characteristics and kinetics of low rank coals by TG-FTIR method. *Fuel Process. Technol.* **2017**, *156*, 454−460.

(48) Zhou, G.; Xu, C.; Cheng, W.; Zhang, Q.; Nie, W. Effects of oxygen element and oxygen-containing functional groups on surface wettability of coal dust with various metamorphic degrees based on XPS experiment. *J. Anal. Methods Chem.* **2015**, *2015*, No. 467242.

(49) Su, X.; Ding, R.; Zhuang, X. Characteristics of dust in coal mines in central North China and its research significance. *ACS Omega* **2020**, *5*, 9233−9250.

(50) Lu, J.; Ren, L.; Rong, D.; Guo, X. Assessment of coal mine gas explosion risk based on grey-matter element model. *China Saf. Sci. J.* **2021**, *31*, 99−105.

(51) Liao, X.; Wang, L.; Zhu, J.; Chu, P.; Liu, Q.; Yang, T. Experimental study on the wettability of tectonic soft coal in Huaibei Mining Area, China. *Energy Fuels* **2021**, *35*, 6585−6599.

(52) Xia, A.; Liu, J. *Mathematical Modeling and MATLAB Application*; Beijing University of Technology Press: Beijing, 2016; p 128.

(53) Zhou, P.; Yao, Y.; Ai, Y.; Liu, A.; Xu, Z.; Xie, J. Grey correlation analysis of factors influencing maldistribution in feeding device of copper flash smelting. *J. Cent. South Univ.* **2012**, *19*, 1938−1945.